Quantum dynamics of electronic excitations in biomolecular chromophores: role of the protein environment and solvent

Joel Gilmore and Ross H. McKenzie

Department of Physics, University of Queensland, Brisbane 4072 Australia
(Dated: February 1, 2008)

We consider continuum dielectric models as minimal models to understand the effect of a surrounding globular protein and solvent on the quantum dynamics of electronic excitations in a biological chromophore. For these models we derive expressions for the frequency dependent spectral density which describes the coupling of the electronic levels in the chromophore to its environment. The magnitude and frequency dependence of the spectral density determines whether or not the quantum dynamics is coherent or incoherent, and thus whether on not one can observe quantum interference effects such as Rabi oscillations. We find the contributions to the spectral density from each component of the chromophore environment: the bulk solvent, protein, and water bound to the protein. The relative importance of each component to the quantum dynamics of the chromophore is determined by the time scale on which one is considering the dynamics. Our results provide a natural explanation and model for the different time scales observed in the spectral density extracted from the solvation dynamics probed by ultra-fast laser spectroscopy techniques such as the dynamic Stokes shift and three pulse photon echo spectroscopy. Our results are used to define under what conditions the dynamics of the excited chromophore is dominated by the surrounding protein and when it is dominated by dielectric fluctuations in the solvent. We show that even when the chromophore is shielded from the solvent by the protein ultra-fast solvation can be dominated by the solvent. Hence, we suggest that the ultra-fast solvation recently seen in some biological chromophores should not necessarily be assigned to ultra-fast protein dynamics. The magnitudes of the spectral density that we estimate from our continuum models and extracted from experiment suggest that most quantum dynamics of electronic excitations is incoherent. A possible exception is transfer of excitons between neigbouring chromophores in photosynthetic systems.

I. INTRODUCTION

The functionality of many proteins is associated with a small subsystem or active site such as a heme group, a couple of amino acids involved in proton transfer, or a co-factor such as an optically active molecule (chromophore). There are a diverse range of optically active molecules that have an important biological function [1]. Examples include retinal (involved in vision), green fluorescent protein and porphyrins (photosynthesis). For these chromophores, the protein acts as a transducer which converts optical excitation of the chromophore into a change such as an electrical signal or conformational change that in turn brings about the desired biological function. Many of these transducers operate with speeds, specificities, and efficiencies which nanotechnologists are striving to mimic [2].

The dynamics of a protein involves thousands of degrees of freedom and at room temperature can be described by classical mechanics and modelled using molecular dynamics methods. In contrast, the functional subsystem involves only a few quantum states and their dynamics must be described quantum mechanically. This has led to considerable effort at developing hybrid QM/MM (quantum mechanical-molecular mechanical) methods [3, 4]. In most cases the change in quantum state associated with the functional event (e.g., transition to an excited electronic state) is associated with a change in the electric dipole moment of the subsystem. Since the protein contains polar residues and is surrounded by a highly polar solvent (water)[5, 6, 7, 8] there is a strong interaction between the functional subsystem and its environment. Consequently, the environment can have a significant effect on the quantum dynamics of the subsystem. Indeed chromophores such as retinal, Photoactive Yellow Protein[4], Green Flourescent Protein exhibit distinctly different dynamics in solution, in the gas phase, and in the protein environment.[9, 10] For example, the speed, efficiency, and selectivity with which excited retinal undergoes a conformational change are all significantly less in water than in the protein environment. [7, 11, 12] This interplay between quantum and classical dynamics raises a number of questions of fundamental interest. On what length and time scales does the crossover from quantum to classical behaviour occur? When are quantum mechanical effects such as coherence (i.e., superposition states), entanglement, tunneling, or interference necessary for biological function?[13, 14] What aspects and details of the structure and dynamic properties of the protein are crucial to biological function?
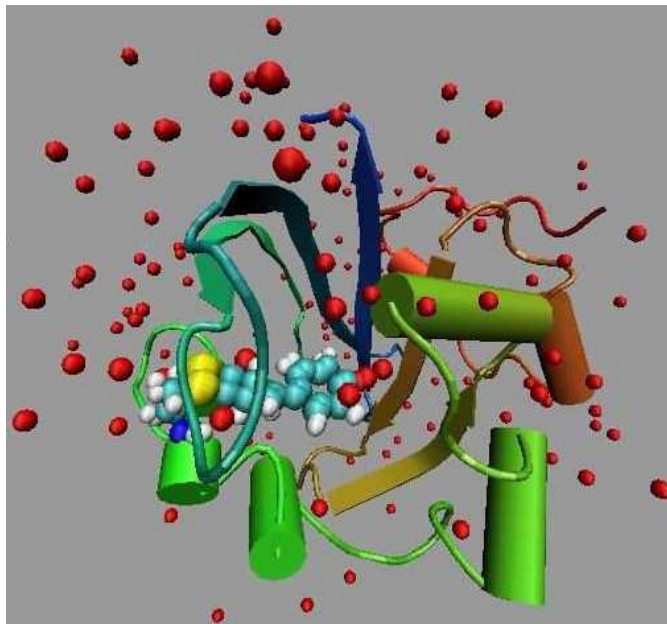
FIG. 1: The chromophore, protein and bound water in photoactive yellow protein (PYP). The isolated spheres represent the bound water, the chromophore is shown by its van de Waals surface, and the protein by a cartoon representation. Observe that the protein surrounding the chromophore reduces the contact of the chromophore with the surrounding bulk water. Generated from the Protein Database 3PYP.pdb[24].

A. Biomolecular chromophores

Most chromophores are large conjugated organic molecules which are surrounded by a protein which in turn is surrounded by a solvent. Figure 1 shows the photoactive yellow protein (PYP), including the chromophore and the so-called "bound water" molecules which reside with comparatively long lifetimes on the surface of the protein [15]. Most chromophores have large dipole moments which change significantly upon optical excitation, leading to significant relaxation of the polarisable environment. Combined chromophore-protein-solvent systems exhibit a broad range of time, length and energy scales (see Figure 2). Typical values of different time scales are shown in Table 1 in the Appendix.

In this paper, we focus on minimal model Hamiltonians, since we are seeking to understand general qualitative features, identify crucial parameters for understanding qualitative changes in behaviour. We specifically consider chromophores which can be described as two level systems (TLS), e.g., we only need consider the ground and first excited state. The models proposed here can also be extended to include internal nuclear dynamics of the chromophore, such as conformational change [6].

Questions of quantum coherence and the role of the environment are particularly pertinent and controversial in photosynthetic systems [16, 17, 18, 19]. It has sometimes been claimed that the excitons within the light harvesting rings are quantum mechanically coherent over some or all of the chromophores (sometimes as many as 32) within the ring. It has also been suggested that such coherence is important for optimum performance of the system[20, 21, 22]. On the other hand, inter-ring transfer of excitons is incoherent which ensures the desirable feature of irreversible transport of energy towards the reaction centre. Recently, the question of delocalisation of excitons over several base pairs in DNA has be studied, motivated by a desire to understand UV damage of DNA.[23]

B. Quantum dynamics, decoherence, and the spin-boson model

Understanding, the dynamics of a quantum system which is strongly coupled to its environment is a challenging theoretical problem that has attracted considerable attention over the past few decades [34]. Many consider that decoherence is the key to resolving the quantum measurement problem.[35, 36, 37] These issues are receiving renewed interest because decoherence is detrimental to quantum information processing.[38, 39] Substantial progress has been made by considering the simplest possible models such as the spin boson model [34] which describes a two-level system
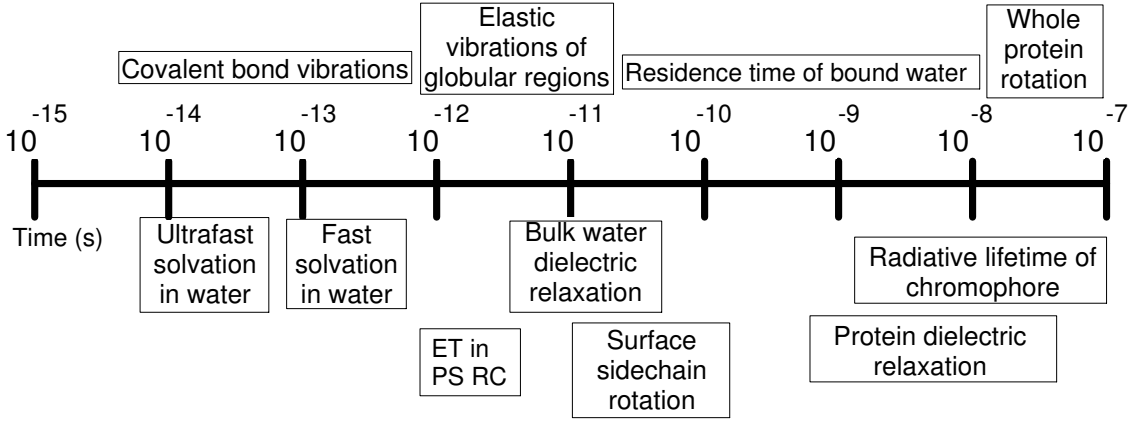
FIG. 2: Schematic representation of the time scales of various processes in proteins and solutions. ET stands for electron transfer, PS RC for photosynthetic reaction centre. Specific numbers and references can be found in the Appendix.

TABLE I: Comparison of the matrix element Δ which couples two quantum states for various processes in proteins with the solvation rates due to the interaction of the quantum system with different parts of its environment. The quantum dynamics of the process will be determined largely by the part of the environment which undergoes solvation relaxation at a rate comparable to Δ. LHI and LHII refer to light harvesting complexes I and II in photosynthetic purple bacteria.

Process	Δ energy (meV)	Ref.
Förster coupling between chromophores in FRET spectroscopy	0.2-2	
Interring Förster coupling between chromophores in LHI and LHII	0.3	[20]
Intraring Förster coupling between two chlorophyl molecules in LHI	50-100	[20]
Förster coupling between infrared amide modes in proteins	0.1-1	[25]
Electron transfer in photosynthetic reaction centre (PRC)	1-10	[26]
Electron transfer in PRC radical cation	10-100	[27]
Electron transfer in proteins	$10^{-4} - 10^{-2}$	[28]
Proton transfer	0.05	[29]
Level crossing for non-radiative decay	40	[30]
Solvation rate due to bulk water	10	[31]
Solvation rate due to bound water	0.1-1	[32]
Solvation rate due to protein	0.004-0.04	[33]

(the "spin")which is coupled linearly to an infinite "bath" of harmonic oscillators.

For biomolecular systems, the spin-boson model has previously been applied to electron transfer.[3, 40, 41] We have recently shown the relevance of the spin-boson model to understanding the effect of the environment on Förster resonant energy transfer between two chromophores[5]. Of particular interest is the case where two molecules are coupled by Resonance Energy Transfer (RET), such as rings of chlorophyll molecules in photosynthesis and in Fluorescent Resonance Energy Transfer spectroscopy (FRET). Here, an excitation in one chromophore may be transferred to a nearby chromophore by the Coulomb interaction, typically dipole-dipole interactions. A coupled system of molecules such as this may be mapped to the spin-boson model [6], where the two quantum states refer to the location of the excitation, ϵ is the difference in the two chromophore's excited energy levels, and $J(\omega)$ describes the coupling of the excitation to the environments surrounding each molecule. We have previously shown [6] that the appropriate spectral density is simply the sum of the spectral density of each individual chromophore-protein complex. The magnitude of the spectral density then determines whether the transfer is coherent (oscillatory) or incoherent (one-way). There are several definite experimental signatures of the coherent interaction of a pair of chromophores. These include (Davydov) splitting of energy levels [42], super- and sub-radiance (i.e., increase and reduction of the radiative lifetime[22, 43]) and changes in fluorescence anisotropy[44]. Both coherence (within a ring) and incoherence (between rings) may play potentially important functional roles in light harvesting complexes.

The Hamiltonian. For the oscillators this can be written as

$$H_0 = \sum_\beta \left(\frac{p_\beta^2}{2m_\beta} + \frac{1}{2} m_\beta \omega_\beta^2 q_\beta^2 \right) \tag{1}$$

where β is an index denoting a particular oscillator with mass m_β, frequency ω_β, momentum p_β, and position q_β. We introduce second quantised operators a_β and $a_\beta^\dagger$ where $a_\beta \equiv \sqrt{\frac{m_\beta \omega_\beta}{2\hbar}}(q_\beta + ip_\beta/(m_\beta \omega_\beta))$, and satisfy the boson commutation relations $[a_\beta, a_\gamma^\dagger] = \delta_{\beta,\gamma}$

The Hamiltonian of the whole system is

$$H = H_0 + H_2 \tag{2}$$

where

$$H_2 = \begin{pmatrix} \frac{\epsilon}{2} + \sum_\beta C_\beta \sqrt{\frac{2m_\beta \omega_\beta}{\hbar}} q_\beta & \Delta \\ \Delta & -\frac{\epsilon}{2} - \sum_\beta C_\beta \sqrt{\frac{2m_\beta \omega_\beta}{\hbar}} q_\beta \end{pmatrix} \tag{3}$$

In terms of the second quantised operators this can be written

$$H = \frac{1}{2}\epsilon\sigma_z + \Delta\sigma_x + \sum_\beta \hbar\omega_\beta a_\beta^\dagger a_\beta + \sigma_z \sum_\beta C_\beta (a_\beta^\dagger + a_\beta), \tag{4}$$

where σ_x and σ_z are Pauli spin matrices, the C_β describes the coupling of the system to each bath mode β, ϵ is the separation of system energy levels and Δ is the tunneling matrix element coupling the two states. Another model is the spin-bath model [45], where the system of interest is coupled to specific localised states of the environment, themselves treated as two level systems.

Spectral density. For the spin-boson model, the quantum dynamics of the two-level system (TLS) is completely determined by a single function, the spectral density,[34] which is defined by

$$J(\omega) = \frac{4\pi}{\hbar} \sum_\beta C_\beta^2 \delta(\omega - \omega_\beta). \tag{5}$$

It describes how strongly the oscillators with frequency near ω are coupled to the two-level system. An important quantity is the *reorganisation energy* defined by,

$$E_R = \int_0^\infty d\omega \frac{J(\omega)}{\omega}. \tag{6}$$

Many systems are described by *ohmic dissipation*, for which $J(\omega) = \hbar\alpha\omega$, below some cutoff frequency, ω_c, related to the relaxation rate of the environment, and if $\Delta \ll \hbar\omega_c$ then at frequencies higher than this cutoff the coupling to the bath of oscillators can be neglected. The main purpose of this paper is to derive physically realistic expressions for this spectral density that are relevant to biological chromophores interacting with their environment.

Known results. If $\epsilon, \Delta \ll \hbar\omega_c$, for ohmic dissipation α is a critical parameter for determining the qualitative properties of the quantum dynamics [34, 46]. At zero temperature, for $\alpha < \frac{1}{2}$ the state of the TLS, exhibits damped Rabi oscillations, a signature of quantum coherence and interference. This can be described by considering the time dependence of the probability that the system is in one of the two levels, which can be related to the expectation value $\langle\sigma_z(t)\rangle$. For $\frac{1}{2} < \alpha < 1$, the system exhibits incoherent relaxation (exponential decay of $\langle\sigma_z(t)\rangle$, and for $\alpha > 1$ the system is localised in its initial state - an example of the quantum Zeno effect [47]. A non-zero temperature reduces the range of α over which coherent oscillations can occur (see Fig. 21.2 in [34]).

If $\Delta > \hbar\omega_c$ then the results of Refs. [34] and [46] do not apply [48]. The bath responds slower than the relevant timescale for the dynamics of the TLS. Consequently, in order to destroy coherent oscillations, the bath must couple more strongly to the two-level system than for the case $\Delta \ll \hbar\omega_c$. System dynamics has been studied with quantum Monte Carlo simulations[49] when $\epsilon = 0$. Coherent oscillations in $\langle\sigma_z(t)\rangle$ may be present for $\alpha > 1$. Fig. 13 in Ref. [49] shows that when $\Delta = 6\hbar\omega_c$ then coherent oscillations can exist even for $\alpha = 30$. Fig. 8 of Ref. [50] shows that for $\Delta = \hbar\omega_c$, numerical renormalisation group calculations predict that coherent oscillations exist for $\alpha < 1.5$. Fig. 3 of Ref. [51] shows that a renormalisation flow equation approach predicts that when $\Delta/\hbar\omega_c$ increases from very small values to 0.3 that the allowed parameter range for coherent oscillations increases to $\alpha < 1.5$. The coherent-incoherent

transition is associated with the delocalisation-localisation transition that has been studied widely in chemistry in systems such as the Creutz-Taube ion and the special pair in photosynthetic systems.[27]

The quantum dynamics of the spin boson model (4) for a general spectral density $J(\omega)$ will be largely determined by the magnitude and frequency dependence of $J(\omega)$ for $\omega \sim \Delta$. For example, when the bath is weakly coupled (i.e., $J(\Delta) \ll \Delta$) to an unbiased ($\epsilon = 0$) two level system coherent oscillations exist, and the relevant decoherence rate given by Fermi's Golden Rule is[34]

$$\frac{1}{T_2} = J(\Delta) \coth\left(\frac{\Delta}{2k_B T}\right).$$ (7)

C. The chromophore environment: protein, bound water, and bulk water

The structures and dynamics associated with the interaction of proteins with water is extremely rich and a challenge to model and to understand.[7, 8, 52, 53]. One can classify the water molecules associated with proteins into several categories. (i) Water which is distant from the protein and has the same properties as bulk water. (ii) Water at the surface of the protein molecule. The first layer of molecules is referred to as the first hydration or solvation layer. These molecules are weakly bound to the charged residues found at the protein surface. (iii) Water buried inside the protein and which often binds to specific sites in the protein via multiple hydrogen bonds. The water inside and at the surface of the protein can exchange with the bulk water.

Advances in experimental probes such as neutron scattering[52], nuclear magnetic resonance (NMR)[8], femtosecond laser spectroscopy,[53] and dielectric dispersion [54] has allowed a quantitative description of the properties of the water molecules associated with specific parts of the solvated protein. Key quantities that can be determined include, (a) the occupancy (i.e., the probability that a water molecule will be found at the site), (b) the residence time (the timescale for exchange of the water molecule with the surrounding bulk water), and (c) the "order parameter" which is a measure of the rotational freedom of the water molecule at the site. NMR measurements suggest that the molecules at the surface exchange with the bulk water on timescales ranging from 10 psec to 1 nsec[8]. In contrast, buried molecules exchange with the solvent on timescales of the order of 1 ns to 1 μs [8].

The term "biological water" has been used to describe water in proximity to a biological macromolecule [55]. Dielectric relaxation is significantly different in biological water [56]. Whereas in bulk water the dominant dielectric relaxation time is 8.3 ps, for bound water this can be 2 to 4 orders of magnitude larger. Dielectric spectroscopy measurements of proteins in aqueous solutions found four dielectric relaxation times.[54] For myoglobin these times were attributed to (1) reorientation of bulk water (8 ps), (2) relaxation of water associated with the protein (10 ps and 150 ps), and (3) reorientation of the whole protein molecule (15 nsec).

Given the structural, chemical, and dynamical complexity of these environments we briefly discuss the limitations of some of the underlying simplications and approximations we assume in our models. Although, these simplifications may lead to quantitative differences between the predictions of our models and real systems we do not anticipate qualitative differences.

Spherical symmetry. We assume that the chromophore is located at the centre of a spherical cavity inside a spherical protein. Similar assumptions have been made in some other studies of dielectric relaxation in proteins.[57, 58] It has been found[59] that there are only small quantitative differences between the dielectric relaxation associated with elliptical cavities compared to spherical ones. Clearly our results will be most relevant to globular proteins with a chromophore towards the centre. A more serious concern is that some chromophores can be located near the protein surface and so more exposed to the solvent. They may be better modelled by a spherical vacuum cavity at the planar interface between two different dielectric medium. Similar geometric considerations apply to transmembrane photosynthetic proteins and systems containing lipid membranes. The approach used here could be extended to such cases by considering continuum dielectric models with different geometries.[60, 61]

Point dipole approximation. The chromophore is treated as a point dipole and its spatial extent is neglected. More realistic treatments of spatially extended distributions inside solvent cavities,[60] do not lead to qualitatively different behaviour.

Neglect of the nuclear dynamics of chromophore. Most electronic transitions will be associated with some structural change of the chromophore. Except, for the case of chromophores (such as retinal and PYP) which undergo conformational change upon photo-excitation, generally the reorganisation energy (and associated Stokes shifts) for modes with frequencies less than 1000 cm^{-1} are typically of order of 10's cm^{-1} and so much smaller than those associated with the solvent and protein.[62]. Furthermore, intra-molecular vibrations with substantial reorganisation energies have sufficiently high frequencies that they occur on timescales much faster than most of the experiments we consider and are not thermally excited at room temperature.

D.   Overview of the paper

In this paper we consider five distinct dielectric continuum models of the environment of a biological chromophore. For each model we derive an expression for the spectral density (5). This allows us to explore how the relative importance of the dielectric relaxation of the solvent, bound water, and protein depends on the relevant length scales (the relative size of the chromophore, the protein and the thickness of the layer of bound water) and time scales (the dielectric relaxation times of the protein, bound water and the solvent) as is discussed in Section V. Many experimentally obtained spectral densities can be fitted to a sum of Lorentzians (see Table II). For a protein that is large compared to the size of the binding pocket of the chromophore and the width of the bound water layer, our models predict a spectral density given by the sum of three Lorentzians which correspond to the dynamics of the protein, bound water and bulk water dynamics respectively. An essential feature is the separation of time scales, associated with the solvation coming from each of the three components of the environment.

Specifically, to a good approximation, the spectral density is given by,

$$J(\omega) = \frac{\alpha_p \omega}{1 + (\omega \tau_p)^2} + \frac{\alpha_b \omega}{1 + (\omega \tau_b)^2} + \frac{\alpha_s \omega}{1 + (\omega \tau_s)^2}. \tag{8}$$

The subscripts $x = p, s, b$ refer to the protein, solvent and bound water, respectively. We show that when the dielectric relaxation of the different components of the environment are treated in a Debye approximation, that the relaxation times can be expressed as:

$$\frac{\tau_p}{\tau_{D,p}} = \frac{2\epsilon_{p,i} + 1}{2\epsilon_{p,s} + 1} \tag{9}$$

$$\frac{\tau_s}{\tau_{D,s}} = \frac{2\epsilon_{s,i} + \epsilon_{p,i}}{2\epsilon_{s,s} + \epsilon_{p,i}} \tag{10}$$

$$\tau_b = \tau_{D,b} \tag{11}$$

where $\epsilon_{x,s}, \epsilon_{x,i}, \tau_{D,x}$ are, respectively, the static dielectric constant, high frequency dielectric constant, and relaxation times of a Debye model for each medium, $x = p, s, b$. The high frequency dielectric constant is related to the refractive index n_x, by $\epsilon_{x,i} = n_x^2$.

We show that the reorganisation energies associated with each part of the environment are given by α_x/τ_x, where

$$\frac{\alpha_p}{\tau_p} = \frac{3(\Delta\mu)^2}{\pi\epsilon_0 a^3} \frac{(\epsilon_{p,s} - \epsilon_{p,i})}{(2\epsilon_{p,s} + 1)(2\epsilon_{p,i} + 1)} \tag{12}$$

$$\frac{\alpha_s}{\tau_s} = \frac{3(\Delta\mu)^2}{\pi\epsilon_0 b^3} \frac{(\epsilon_{s,s} - \epsilon_{s,i})}{(2\epsilon_{s,s} + \epsilon_{p,i})(2\epsilon_{s,i} + \epsilon_{p,i})} \left(\frac{9\epsilon_{p,i}}{(2\epsilon_{p,i} + 1)^2} \right) \tag{13}$$

$$\frac{\alpha_b}{\tau_b} = \frac{3(\Delta\mu)^2}{2\pi\epsilon_0 b^3} \left(\frac{c - b}{b} \right) \frac{(\epsilon_{b,s}^2 + 2\epsilon_{s,s}^2)(\epsilon_{b,s} - \epsilon_{b,i})}{\epsilon_{b,s}^2 (2\epsilon_{s,s} + \epsilon_{p,i})^2} \tag{14}$$

In particular, for typical systems the above three quantities can be of the same order of magnitude, i.e.,

$$\frac{\alpha_s}{\tau_s} \sim \frac{\alpha_b}{\tau_b} \sim \frac{\alpha_p}{\tau_p}. \tag{15}$$

Due to the large separation of time scales, the spectral density (8) will have peaks at approximately, $\omega = 1/\tau_x$. Hence, the peaks are of approximate magnitude, $J(\omega = 1/\tau_x) \sim \alpha_x/\tau_x$, and can be of the same order of magnitude. This is because although each contribution involves different dielectric constants, they only have a limited range of values, and the ratios of the different dielectric constants that appear on the right hand side of the above expressions are all of order one. This is supported by experimental data (see Table II) where several relaxation times are observed which vary by several orders of magnitude, but whose relative contributions are of comparable magnitude. Hence, in many cases only a single component of the environment (protein, bound water, or bulk solvent) will be relevant to a given process.

The effect of the protein. The expression (13) allows us how the ultra-fast solvation associated with the solvent is modified in the presence of a protein. Water is a highly polar medium with $\epsilon_{s,s} \simeq 80$, and $\epsilon_{s,i} \simeq 4$, and fast dielectric relaxation, $\tau_{D,s} \simeq 8$ psec. Hence, we see that even if $\epsilon_{p,i}$ is as large as 5 that the solvation time associated with the solvent is only be 50 per cent larger compared to the time of 0.3 psec which occurs in the absence of the protein. The effect of the protein on the strength of the coupling of the chromophore to the solvent is more substantial. In (13), the coupling scales with the inverse cube of the power of the radius of the protein. Hence, if the diameter of the protein is four times the size of the chromophore, the coupling α_s will be reduced by two orders of magnitude. The above results show that even a distant solvent can lead to ultra-fast solvation comparable to that found in the absence of the protein. This leads us to suggest that some studies which claim to have identified ultra-fast dielectric relaxation of proteins [63, 64] may in fact be detecting the fast response of the distant solvent.

Order of magnitude estimates of α_x. Typical values of parameters are $a \sim 3\mathring{A}$, $b \sim 10\mathring{A}$, $\Delta\mu \sim 1D$, and so the reorganisation energy $\alpha_x \hbar/\tau_x \sim 10$ meV ~ 100 cm^{-1}. From Figure 2 and the Table in the Appendix we see that $\hbar/\tau_x$ is of the order of 10 meV, 1 meV, and 0.01 meV, for the solvent, bound water, and protein, respectively. Hence, the dimensionless couplings $\alpha_s \sim 1$, $\alpha_b \sim 10$, and $\alpha_p \sim 100$. Hence, the only quantum dynamics that is likely to be coherent is that which occurs on timescales comparable to or faster than the relaxation of the bulk water, i.e., less than a picosecond.

The outline of the paper is as follows. In Section II we describe how the interaction between a chromophore and its protein and solvent environment may be modelled by an independent boson model. We show how the interaction with the environment leads to decoherence of the electronic states of the chromophore. In Section III we propose a set of continuum dielectric models suitable for describing the environment around a chromophore, and use them to obtain an expression for the spectral density in each case. In Section IV we consider particular limits of these spectral densities and obtain simple expressions for the contribution of each component of the environment (protein, bound water, and bulk water) to the total spectral density. In particular, we are able to obtain expressions that can be used to evaluate the relative importance of each component of the environment. We find that even when the chromophore is completely surrounded by a protein it is possible that the ultra-fast solvation (on the psec timescale) is dominated by the bulk solvent surrounding the protein. In Section V we discuss methods for obtaining spectral densities from optical spectroscopy, and compare the predictions of our models to experimental data. In Section VI we relate our results for the spectral density due to dielectric relaxation to what has been learnt from molecular dynamics simulations on specific protein systems.

II. QUANTUM DYNAMICS OF THE INDEPENDENT BOSON MODEL

It can be shown [6] that the coupling of the electronic excitations in a chromophore to its environment may be modelled by an independent boson model [65], which has the Hamiltonian,

$$H = \frac{1}{2}\epsilon\sigma_z + \sum_\beta \omega_\beta a_\beta^\dagger a_\beta + \sigma_z \sum_\beta C_\beta(a_\beta + a_\beta^\dagger). \tag{16}$$

We note that this is just the spin boson model with $\Delta = 0$. Here the chromophore is treated as a two level system with energy gap ϵ between the ground and excited state. The first term describes the energy of the isolated chromophore, described by Pauli sigma matrix σ_z. The second term is the energy of the surrounding environment (protein and solvent), where the environment is modelled as a bath of harmonic oscillators [6]. The final term describes the coupling of the state of the chromophore σ_z to the environment. In this case, the coupling [66, 67] is due to electrostatic interactions between the chromophore dipole and the "cage" of polarised solvent and protein molecules around it, as will be described in more detail below. The effect of this coupling on the quantum dynamics of the chromophore is completely specified by the spectral density, defined by eq. (5) [65].

If the two-level system is initially ($t = 0$) in a coherent superposition state $|\Psi> = a|1> + b|2>$, which is not coupled to the environment. An ultra-fast laser pulse can create such a state. Then at time t, the TLS is described by a 2×2 reduced density matrix, $\rho(t)$. It has matrix elements [68]

$$\rho_{11}(t) = \rho_{11}(0) = |a|^2$$
$$\rho_{22}(t) = \rho_{22}(0) = |b|^2 = 1 - \rho_{11}(0)$$
$$\rho_{12}(t) = \rho_{21}^*(t) = a^*b \exp(-i\epsilon t + i\theta(t) - \Gamma(t,T)) \tag{17}$$

where $\theta(t)$ is a phase shift given by

$$\theta(t) = \int_0^\infty d\omega J(\omega) \frac{[\omega t - \sin(\omega t)]}{\omega^2} \tag{18}$$

and

$$\Gamma(t,T) = \int_0^\infty d\omega J(\omega) \coth\left(\frac{\omega}{2k_BT}\right) \frac{(1-\cos\omega t)}{\omega^2} \tag{19}$$

describes the decoherence due to interaction with the environment.

The phase shift can be used to define a time dependent Stokes shift of the energy separation of the two levels. The instantaneous energy is found by taking the derivative of (18) with respect to time,[59, 69]

$$\nu(t) = \epsilon - \frac{d\theta(t)}{dt} = \epsilon - E_R - \int_0^\infty d\omega \frac{J(\omega)}{\omega} \cos(\omega t) \tag{20}$$

Hence, the spectral density can be determined by taking the Fourier transform of measurements of $\nu(t)$, as discussed in Section V.

Depending on the relative size of the time t to the time scales defined by $1/\omega_c$ (the relaxation time of the bath) and $\hbar/k_BT$, there are three different regimes of time dependence. For short times $\omega_c t < 1$,

$$\Gamma(t,T) = \frac{t^2}{2\tau_g^2} \tag{21}$$

and so there is a Gaussian decay of coherence, on a time scale τ_g, given by

$$\frac{1}{\tau_g^2} = \int_0^\infty d\omega J(\omega) \coth\left(\frac{\omega}{2k_BT}\right). \tag{22}$$

If in addition, $k_BT \gg \hbar\omega_c$, this reduces to

$$\frac{\hbar}{\tau_g} = \sqrt{2E_R k_BT} \tag{23}$$

where E_R is the reorganisation energy given by Eqn. (6).

For intermediate times, $1/\omega_c < t < \hbar/k_BT$ (the quantum regime [38]; it only exists if $k_BT < \hbar\omega_c$), then

$$\Gamma(t,T) \approx \alpha \ln(\omega_c t), \tag{24}$$

where $\alpha \equiv J'(\omega = 0)$, leading to a power law decay of coherence.

For long times ($t \gg \hbar/k_BT$, the thermal regime)

$$\Gamma(t,T) \approx 2\alpha k_BTt/\hbar \equiv t/\tau_d, \tag{25}$$

giving exponential decay of coherence.

The crossover from Gaussian to exponential decay has been explored in quantum measurement theory in the context of continuous measurement and the quantum Zeno effect [47]. The decay of the off-diagonal part of the density matrix results from decoherence from the interaction of the TLS with the environment. Thus, we see the effect of the environment on the TLS is

$$\rho(t=0) = \begin{pmatrix} |a|^2 & a^*b \\ ab^* & |b|^2 \end{pmatrix} \quad \rightarrow \rho(t \rightarrow \infty) = \begin{pmatrix} |a|^2 & 0 \\ 0 & |b|^2 \end{pmatrix} \tag{26}$$

Hence, the timescale τ_d can be interpreted as the "collapse" of the wavefunction of the TLS due continuous measurement of the state of the TLS by the environment.[36, 37, 47] We will see that using the spectral densities that we extract from experiment and from our continuum dielectric models that typically $\alpha > 1$, and so at room temperature, $\tau_d < 10$ fsec.

III. THE SPECTRAL DENSITY FOR THE DIFFERENT CONTINUUM MODELS OF THE ENVIRONMENT

In the simplest continuum model [57] picture of protein-pigment complexes, the chromophore can be treated as a point dipole inside a spherical dielectric [57, 67], representing a globular protein, surrounded by a uniform polar solvent with complex dielectric constant $\epsilon_s(\omega)$ [66]. This can also apply to a chromophore-protein complex embedded
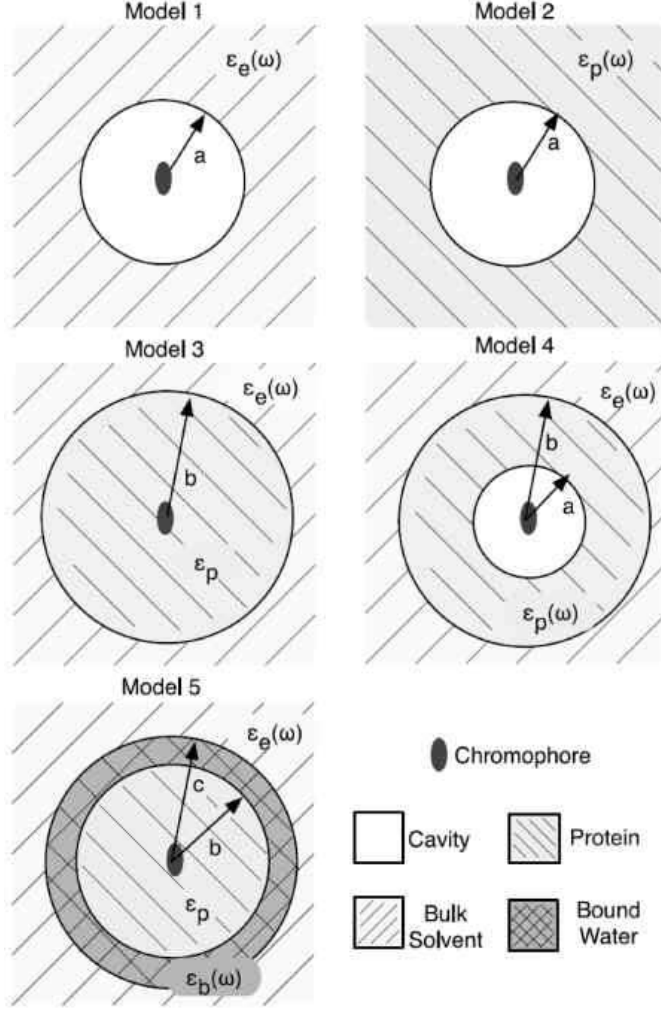
FIG. 3: The five continuum dielectric models considered for a chromophore-protein-solvent system. The chromophore is modelled as a point dipole. In Model 1, the chromophore is modelled sits at the centre of a cavity of radius a roughly of the van de Waals size of the chromophore, surrounded by a uniform polar solvent with complex dielectric constant $\epsilon_s(\omega)$. In Model 2, the chromophore is surrounded by an infinite protein, modelled as a uniform, continuous dielectric medium, with complex dielectric constant $\epsilon_p(\omega)$. In Model 3, the chromophore sits in a protein of radius b surrounded by the solvent. In Model 4, the chromophore sits in a cavity inside the dynamic protein, surrounded by solvent. In Model 5, the static protein is surrounded by a thin shell of bound water of radius c, surrounded by the bulk solvent.

in a solid dielectric medium. In a previous work [6], the spectral density was determined for a free chromophore in a solvent. However, many chromophores are inside proteins, which may have a significant effect on the coupling to the environment, if only in pushing back the solvent.

Several continuum dielectric models for the protein environment have previously been proposed (see for example Figure 2 in ref. [57] and Figure 2 in ref. [70].) These models often provide good qualitative and rough quantitative agreement [58]. We consider five distinct models, illustrated in figure 3. In every case, the central chromophore dipole polarises the surrounding cage of protein and solvent, which in turn produces an electric field inside the cavity, called the *reaction field* [66, 67]. The interaction of this field with the central dipole is responsible for the interaction between the chromophore and its environment. The independent boson model can be obtained by writing the reaction field in terms of its normal modes, and quantising the coefficients in the standard second quantisation method [6], and the fluctuation dissipation theorem used to relate fluctuations in the reaction field to the appropriate spectral density [6]. A detailed derivation applicable to all models considered below, is given in the Appendix.

Model 1. This describes a free chromophore with no surrounding protein. The molecule sits inside a spherical cavity of radius a, approximately the van de Waals radius of the molecule, inside a solvent with dielectric constant

$\epsilon_s(\omega)$. The spectral density is[59]

$$J_1(\omega) = \frac{(\Delta\mu)^2}{2\pi\epsilon_0 a^3}\text{Im}\frac{(\epsilon_s(\omega) - \epsilon_c)}{2\epsilon_s(\omega) + \epsilon_c}. \tag{27}$$

where a is the radius of the cavity containing the chromophore and $\epsilon_s(\omega)$ is the complex dielectric function of the solvent and ϵ_c the (static) dielectric constant of the cavity. $\Delta\mu$ is the difference between the dipole moment of the chromophore in the ground and excited states.

Model 2. This is somewhat analogous situation to Model 1, but in this case the chromophore is surrounded by an infinite, uniform protein with complex dielectric constant $\epsilon_p(\omega)$. This chromophore is again inside a cavity of radius a, which would be approximately the same radius as for Model 1. Such a model may be appropriate when the protein is very large. The spectral density has a similar form to Model 1, except involves the dielectric constant of the protein $\epsilon_p(\omega)$:

$$J_2(\omega) = \frac{(\Delta\mu)^2}{2\pi\epsilon_0 a^3}\text{Im}\frac{(\epsilon_p(\omega) - \epsilon_c)}{2\epsilon_p(\omega) + \epsilon_c}. \tag{28}$$

Model 3. The chromophore is surrounded by a uniform dielectric sphere representing the protein. This protein sphere has radius b and (constant) dielectric constant ϵ_p. The spectral density is

$$J_3(\omega) = \frac{(\Delta\mu)^2}{2\pi\epsilon_0 b^3}\text{Im}\frac{(\epsilon_s(\omega) - \epsilon_p)}{2\epsilon_s(\omega) + \epsilon_p}. \tag{29}$$

where $\epsilon_s(\omega)$ is the complex dielectric function of the solvent.

Model 4. In a more detailed picture, (see the Figure the Appendix), Models 2 and 3 are combined so that the chromophore sits inside a hollow cavity within the protein. The cavity has radius a (typically the size of the chromophore) and vacuum dielectric constant ϵ_0, while the protein again has radius b and is now described by complex dielectric constant $\epsilon_p(\omega)$. Further detail may be added by treating the outer layer of the protein sphere as a separate, higher dielectric medium [57] representing the charged surface groups [71]. In all cases, the chromophore is treated as a point dipole. The spectral density is given by

$$J_4(\omega) = \frac{(\Delta\mu)^2}{2\pi\epsilon_0 a^3}\text{Im}\frac{(\epsilon_p + 2)(\epsilon_s - \epsilon_p)a^3 + (\epsilon_p - 1)(2\epsilon_s + \epsilon_p)b^3}{2(\epsilon_p - 1)(\epsilon_s - \epsilon_p)a^3 + (2\epsilon_p + 1)(2\epsilon_s + \epsilon_p)b^3} \tag{30}$$

where b is the radius of the protein containing the chromophore, a is the radius of the cavity containing the chromophore (usually the size of the chromophore), ϵ_s is the complex dielectric function of the solvent and ϵ_p is now the complex dielectric function of the protein. Note that the frequency dependence of the dielectric constants has been omitted for clarity. We see that for appropriate limits ($(a/b) \to 0$, $\epsilon_p = \epsilon_s$, $\epsilon_p = 1$, etc) Models 1 and 2 can be recovered, as expected. (To obtain Model 3, one would have to allow the centre cavity in Model 4 to have an arbitrary dielectric constant.)

Model 5. The chromophore sits in a static protein (no cavity) and is surrounded by a thin shell of bound water with a different dielectric constant to the bulk solvent. To obtain the spectral density, we can use the results for Model 4, with $\epsilon_p \to \epsilon_b, \epsilon_c \to \epsilon_p, a \to b$, and $b \to c$:

$$J_5(\omega) = \frac{(\Delta\mu)^2}{2\pi\epsilon_0 b^3}\text{Im}\frac{(\epsilon_b + 2\epsilon_p)(\epsilon_s - \epsilon_b)b^3 + (\epsilon_b - \epsilon_p)(2\epsilon_s + \epsilon_b)c^3}{2(\epsilon_b - \epsilon_p)(\epsilon_s - \epsilon_b)b^3 + (2\epsilon_b + \epsilon_p)(2\epsilon_s + \epsilon_b)c^3} \tag{31}$$

Note that ϵ_p refers to a constant (typically high frequency) protein dielectric viz. Model 2. ϵ_b is the complex dielectric of the bound water.

A. Debye model for the frequency dependence of the dielectric constants

To specify the dielectric constant of each component of the environment $\epsilon_x(\omega)$ ($x = s, p, b$) we consider the Debye form of the dielectric constant[59],

$$\epsilon_x(\omega) = \epsilon_{x,i} + \frac{\epsilon_{x.s} - \epsilon_{x,i}}{1 - i\omega\tau_{D,x}} \tag{32}$$

where $\tau_{D,x}$ is the Debye relaxation time of the relevant component, $\epsilon_{x,s} = \epsilon(\omega = 0)$ is the static dielectric constant, and $\epsilon_{,i} = \epsilon(\omega \to \infty)$ is the high frequency dielectric constant, within the range of physically relevant frequencies –

note that $\epsilon_{x,i}$ would always be 1 for sufficiently high frequencies [72]. For water at room temperature, $\epsilon_{s,s} = 78.3$, $\epsilon_{s,i} = 4.21$ and $\tau_{D,s} = 8.2$ ps [73]. For comparison, for THF (tetrahydrofuran) the values are $\epsilon_{s,s} = 8.08$, $\epsilon_{s,i} = 2.18$ and $\tau_{D,s} = 3$ ps [74].

In Model 4, the protein is treated as a complex frequency dependent dielectric with dielectric constant $\epsilon_p(\omega)$, and as such is allowed to relax and respond to the chromophore. We will consider the case of a Debye dielectric [72], but a more complicated model including multiple relaxation times is also possible [75]. Typical values for ϵ_p are between 4–40 depending on which part of the protein is of interest [57, 76, 77]. Studies also suggest that charged groups on the surface of the protein can skew the average value of the protein dielectric, and it may be more appropriate to model such proteins as having an inner and an outer shell with two different dielectric constants. The high frequency constant, which is the only value used by many studies, is more difficult to determine but is generally assumed to be between 1.5 and 2.5 [22, 78]. Section VI discusses determinations of $\epsilon_p(\omega)$ from molecular dynamics simulations.

The appropriate dielectric relaxation time of the protein may be different from the protein relaxation times, which can be of order milliseconds [42], as there are processes (e.g., vibration of bonds) on the order of femtoseconds [42, p132, Table 3.13] which may contribute to the dielectric function. These may be missed in studies of the dielectric constant on the nanosecond timescale [79] and is perhaps unobservable for aqueous solutions of proteins (e.g., ref. [80]). Molecular dynamics simulations [77] suggest a protein dielectric relaxation time of 10 ns for a peptide, while vibrations may be of the order of 100 fs which may apply in certain situations. Other studies have found no single relaxation times, with relaxation processes occurring across the entire experimental range of 20 ps – 20 ns[81, 82].

For Model 3, an appropriate value for the constant dielectric of the protein must be chosen, which will depend on the frequency range of physical interest. For example, for frequencies greater than $1/\tau_p$, where τ_p is approximately the protein dielectric relaxation time, the protein will be well approximated by its high frequency value.

The hydration shell of hydrogen bonded water molecules surrounding the protein will have a dielectric constant different to that of the bulk solvent, and have a longer Debye relaxation time.

IV. ANALYSIS OF MODEL 4 AND MODEL 5

A. Model 4 - Dynamic protein and dynamic solvent

The full spectral density (Model 4) describes the total coupling to the protein and solvent, but is too complex to be written analytically and because of the multiple timescales involved may be non-Ohmic, in certain frequency ranges. However, there are many cases where the use of one of the simpler descriptions (Models 1-3) would be preferable. For example if the frequency dependent dielectric constant of either the protein or solvent were not known, it would be useful to have a simple criteria to establish whether obtaining these parameters is worthwhile. If protein contributes negligible coupling beyond pushing the solvent back to a new distance, then specially obtaining its dielectric through experiment or simulation would be unnecessary.

If either the solvent or the protein can be deemed unimportant, then simulations of the chromophores do not require their inclusion, saving valuable computational power. Conversely, if (for example) the solvent can be shown to have a significant effect on the chromophore, then treating the protein only will be insufficient and solvent effects must be included. Hence, we explore under what conditions the protein dynamics may be neglected. The following discussion assumes that the dielectric relaxation time of the protein is longer than that of the solvent, which is expected to be true in the vast majority of cases.

1. Limit of a small chromophore surrounded by a large protein

In the case of an "infinite" protein $a/b \to 0$, the full spectral density (Model 4) reduces to $J_2(\omega)$, the spectral density for Model 2. In this limit, the solvent can be neglected when compared to the protein. We might naively assume then that, since the ratio a/b appears cubed, when the protein is several times larger than the chromophore the above spectral density can be used and the coupling to the protein is far stronger than to the solvent. However, a closer examination of (30) shows that if $\epsilon_p(\omega) \approx 1$, the solvent will be more significant even for large values of b/a, and a more appropriate expression for the spectral density describes the chromophore in a cavity of radius b surrounded by solvent. Hence, we seek a more precise statement for when the protein can be ignored. The spectral density can be rewritten:

$$J_4(\omega) = \frac{(\Delta\mu)^2}{2\pi\epsilon_0 a^3} \frac{\left(\frac{\epsilon_p+2}{2\epsilon_p+1}\right)\left(\frac{\epsilon_s-\epsilon_p}{2\epsilon_s+\epsilon_p}\right)\frac{a^3}{b^3} + \left(\frac{\epsilon_p-1}{2\epsilon_p+1}\right)}{\left(\frac{2(\epsilon_p-1)}{2\epsilon_p+1}\right)\left(\frac{\epsilon_s-\epsilon_p}{2\epsilon_s+\epsilon_p}\right)\frac{a^3}{b^3} + 1}$$

(33)

We can expand this expression in $\frac{\epsilon_s - \epsilon_p}{2\epsilon_s + \epsilon_p}\frac{a^3}{b^3}$. Note that although this is a complex quantity, provided both the real and imaginary parts are small compared to unity we can use the Taylor series expression $\frac{ax+b}{cx+1} \approx b + (a - bc)x$. Furthermore, both the real and imaginary parts of the prefactor of this expansion coefficient will be less than unity, and a sufficient condition for this expansion to be valid is that a/b be small. We find

$$J_4(\omega) \approx J_2(\omega) + \frac{(\Delta\mu)^2}{2\pi\epsilon_0 b^3}\text{Im}\left[\frac{\epsilon_s(\omega) - \epsilon_p}{2\epsilon_s(\omega) + \epsilon_p}\right]\left(\frac{9\epsilon_p}{(2\epsilon_p + 1)^2}\right)$$
$$= J_2(\omega) + J_s(\omega) \tag{34}$$

where $J_s(\omega)$ represents the solvent contribution to the spectral density. Note that the dynamics of the protein only contribute to the first term, which conversely contains no reference to the solvent. The second term includes the solvent dynamics plus the high frequency limit of the protein dielectric constant as the only relevant protein property. Thus, we identify the first term with the protein contribution and the second term with the solvent, modified by the presence of the protein's high frequency dielectric.

2. Relevance of protein vs. solvent

By comparing the magnitudes of these two terms in (34), we can establish the relative importance of the solvent and protein over different frequency ranges. We might expect that around $\omega = 1/\tau_p$ and $\omega = 1/\tau_s$ that the protein and solvent contributions should dominate respectively. Therefore, there should be a crossover point where the two contributions are roughly equal, somewhere in the range $1/\tau_p \ll \omega \ll 1/\tau_s$, which is what we look for now.

As defined above, the cut-off frequency of $\omega_p = 1/\tau_p$. Assuming a Debye dielectric for the protein, eq. (28) can be approximated to first order in ω_p/ω as:

$$J_2(\omega) \approx \omega_p^2\alpha_p/\omega, \qquad \omega \gg \omega_p \tag{35}$$

Therefore, the tail end of the spectral densities given fall off as $1/\omega$ (as compared to their linear rise for $\omega \ll \omega_p$). Noting that the reorganisation energy for this spectral density is $E_p = \alpha_p\omega_p$, we write the spectral density for $\omega \gg \omega_p$ as $J_2(\omega) = E_p\omega_p/\omega$. (This is quite different to the spectral density for $\omega \ll \omega_p$, which is $J(\omega) = E_p\omega/\omega_p$.)

The second term in (34) is somewhat more difficult to evaluate. We will again Taylor expand in $1/(\tau_p\omega)$. We note, however, that by extracting a factor of $1/a^3$ from both terms of (34) the second term is proportional to $(a/b)^3$, which we already assumed is "small" in the first Taylor expansion. Therefore, when we again Taylor expand around ω_p/ω we need only work to zeroth order so that our total final approximation for $J_4(\omega)$ is to first order in two small expansion variables. This yields,

$$J_s(\omega) \approx \frac{9\epsilon_{p,i}}{(2\epsilon_{p,i} + 1)^2}J_3(\omega) \tag{36}$$

where $J_3(\omega)$ is the spectral density for Model 3, with $\epsilon_p \equiv \epsilon_{p,i}$, i.e., the chromophore inside a constant dielectric (high frequency) protein with no cavity, surrounded by the solvent. The solvent contribution is therefore ohmic, with a dimensionless coupling constant, α_s given by (13).

Therefore, equating the two spectral densities suggests a crossover between solvent and protein dominance at frequency ω_{co},

$$\frac{\omega_{co}}{\omega_{pe}} = \sqrt{\frac{\alpha_p}{\alpha_s}} \tag{37}$$

This ratio is always much larger than one for typical values of dielectric constants and relaxation times.

For frequencies above this limit, provided we are in the regime $b \gg a$, we would expect that the protein dynamics are irrelevant for the system, and the dynamics of the chromophore is "slaved" to the solvent fluctuations. Similar effects have been observed in enzyme kinetics[83]. At low frequencies ($\omega \ll \omega_{co}$), the protein dynamics dominate and the details of the solvent are mostly irrelevant. Hence, we expect that even when the chromophore is "shielded" from the solvent by the protein that the short time (~ 1 psec) dynamics can still be dominated by the solvent. This raises questions about the recent assignment of the observed ultra-fast solvation to protein dynamics.[63, 64, 84]

B. Model 5 - Bound water

Our goal is to obtain analytic criteria which tell us when the bound water is relevant. If the dielectric contribution of the bound water dominates over that of the protein, we can use Model 5 to describe the system. Instead of

the chromophore pocket being treated as the cavity, now the entire protein is treated as a cavity of radius b with frequency-independent dielectric ϵ_p. This is surrounded by a shell of bound water with radius c (so the shell has width $c-b$) and dielectric $\epsilon_b(\omega)$ (with the subscript representing the bound water). We expect that the layer of bound water (typically [15] about 4.5Å) will be thin compared to the rest of the protein ($b \sim 20$Å), and so we are interested in the limit $b \approx c$.

We simplify the spectral density (31) in the same way as Section IV A. The full details may be found in the Appendix. Taylor expanding in $\frac{c-b}{b}$ yields

$$J_5(\omega) = J_3(\omega) + J_{\mathrm{bw}}(\omega) \tag{38}$$

The first term represents the spectral density of a chromophore inside a cavity of radius b with dielectric constant ϵ_p surrounded by a bulk solvent, and so is the spectral density in the absence of the bound water, as described by Model 3. The second term, is proportional to the ratio $\frac{c-b}{b}$, a measure of the thickness of the bound water, and can be identified with the contribution to the spectral density of the bound water:

$$J_{\mathrm{bw}}(\omega) = \frac{2}{\epsilon_b} \left(\frac{2\epsilon_s + \epsilon_b}{2\epsilon_s + \epsilon_p} \right)^2 \left(\frac{\epsilon_b - \epsilon_s}{2\epsilon_s + \epsilon_b} \right) \frac{(c-b)}{b} \tag{39}$$

Then, the bound water term can be expressed as

$$J_{\mathrm{bw}}(\omega) \approx \frac{1}{(2\epsilon_s + \epsilon_p)^2} \mathrm{Im} \left[\left(1 + \frac{2\epsilon_{s,s}}{\epsilon_b} \right) (\epsilon_b - \epsilon_{s,s}) \right] \tag{40}$$

$$= \frac{1}{(2\epsilon_s + \epsilon_p)^2} \left(1 + \frac{2\epsilon_{s,s}^2}{|\epsilon_b(\omega)|^2} \right) \mathrm{Im}\epsilon_b(\omega) \tag{41}$$

Using a Debye form for the bound water spectral density, gives $\mathrm{Im}[\epsilon_b(\omega)] = (\epsilon_{b,s} - \epsilon_{b,i})\frac{\omega\tau_b}{1+\omega^2\tau_b^2}$. However, we must also include the $|\epsilon_b(\omega)|^2$ contribution to the frequency dependence. If we consider frequencies much less than the bulk solvent relaxation time $1/\tau_s$, then we again find an ohmic spectral density for the bound water contribution, with dimensionless coupling given by Equation (14).

In comparison with the solvent contribution,

$$\frac{\alpha_b}{\alpha_s} \approx \left(\frac{c-b}{b} \right) \frac{\tau_b}{\tau_s} \frac{\epsilon_{b,s} - \epsilon_{b,i}}{\epsilon_{s,s} - \epsilon_{s,i}} \frac{(\epsilon_{b,s}^2 + 2\epsilon_{s,s}^2)(2\epsilon_{s,i} + \epsilon_p)}{\epsilon_{b,s}^2(2\epsilon_{s,s} + \epsilon_p)} \tag{42}$$

We would typically expect $\epsilon_{s,s} \gg \epsilon_{s,i}$, $\epsilon_{b,s} \gg \epsilon_{b,i}$, and $\epsilon_{s,s} \gg \epsilon_{b,s}$ and the protein static dielectric constant to be small compared to any static frequency, but perhaps comparable to the high frequency values of the dielectric constants of bulk or bound water. Therefore,

$$\frac{\epsilon_{b,s} - \epsilon_{b,i}}{\epsilon_{s,s} - \epsilon_{s,i}} \frac{(\epsilon_{b,s}^2 + 2\epsilon_{s,s}^2)(2\epsilon_{s,i} + \epsilon_p)}{\epsilon_{b,s}^2(2\epsilon_{s,s} + \epsilon_p)} \sim \frac{\epsilon_{b,s}}{\epsilon_{s,s}} \frac{4\epsilon_{s,s}^2\epsilon_{s,i}}{2\epsilon_{b,s}^2\epsilon_{s,s}} \sim \frac{\epsilon_{b,i}}{\epsilon_{b,s}} \tag{43}$$

which we expect to be of order one. Therefore, we would usually expect

$$\frac{\alpha_b}{\alpha_{pe}} \sim \frac{c-b}{b} \frac{\tau_b}{\tau_{pe}} \tag{44}$$

Hence, if $\tau_b \gg \tau_s$, as is observed [107, 108], then we would expect the bound water to be the dominant effect. Further, since the heights of the peaks are approximately given by their reorganisation energy ($J(\omega_c) = \alpha\omega_c \sim E_R$) we find

$$\frac{E_b}{E_s} \sim \frac{c-b}{b} \tag{45}$$

where E_b, E_s are the reorganisation energies of the bound water and solvent respectively.

The cross-over frequency between the bound water and bulk water contributions dominating the spectral density can be estimated by the condition $J_s(\omega_{co}) = J_b(\omega_{co})$. Assuming that the bulk and bound water timescales are sufficiently separated that at the cross-over point $J_b(\omega)$ is in the decaying tail and $J_e(\omega)$ is in the linear region, then the cross-over frequency is given by

$$\frac{\omega_{co}}{\omega_b} = \sqrt{\frac{\alpha_s}{\alpha_b}} \tag{46}$$

V. SPECTRAL DENSITIES DETERMINED FROM ULTRA-FAST OPTICAL SPECTROSCOPY

The spectral function $J(\omega)$ associated with optical transitions in chromophores can be extracted from ultra-fast laser spectroscopy [53, 69, 85]. Two widely used techniques for doing this are the dynamical Stokes shift and three-photon echo spectroscopy.

Dynamical Stokes shift. The time dependence of the Stokes shift in the fluorescence spectrum, where $\nu(t)$ is the maximum (or the first frequency moment) of the fluorescence spectrum at time t, can be normalised as

$$C(t) = \frac{\nu(t) - \nu(\infty)}{\nu(0) - \nu(\infty)} \tag{47}$$

such that $C(0) = 1$, and $C(\infty) = 0$ when the fluorescence maxima has reached its equilibrium value. Using Equation (20) this is related to the spectral density by

$$C(t) = \frac{\hbar}{E_{\mathrm{R}}} \int_0^\infty d\omega \frac{J(\omega)}{\omega} \cos(\omega t) \tag{48}$$

where E_{R} is the total reorganisation energy given in eq. (6), which also equals the total Stokes shift associated with solvation.

The function $C(t)$ is sometimes referred to as the *hydration correlation function* and experimental results are often fitted to several decaying exponentials,

$$C(t) = A_1 \exp(-t/\tau_1) + A_2 \exp(-t/\tau_2) + A_3 \exp(-t/\tau_3) + \ldots \tag{49}$$

where $A_1 + A_2 + \ldots = 1$. From (48), this corresponds to a spectral density of the form

$$J(\omega) = \frac{\alpha_1 \omega}{1 + (\omega \tau_1)^2} + \frac{\alpha_2 \omega}{1 + (\omega \tau_2)^2} + \ldots \tag{50}$$

The dimensionless couplings α_j $(j = 1, 2, \ldots)$ are related to the total reorganisation energy by

$$\alpha_j = \frac{2 E_{\mathrm{R}} A_j \tau_j}{\pi \hbar} \simeq 0.25 A_j \frac{E_{\mathrm{R}}}{cm^{-1}} \frac{\tau_j}{psec}. \tag{51}$$

Table II gives values of the fitting parameters $(E_{\mathrm{R}}, A_j, \tau_j)$ determined by fast laser spectroscopy for a range of chromophores and different environments, both protein and solvent. We do not claim the list is exhaustive of all the published values, but is meant to be indicative (For example, see also [25, 63, 64, 86, 87, 88, 89]) We note the following general features.

(i) The Stokes shift varies significantly between different environments, both solvent and protein. Generally, the presence of the protein reduces the total Stokes shift and the relative contribution of the ultra-fast component, which can be assigned to the solvent. The less exposed the chromophore is to the solvent the smaller is solvent contribution to the spectral density. This is also seen in measurements of the dynamic Stokes shift for a chromophore placed at three different sites in the B1 domain of protein G. (See Fig. 3C of Ref. 90). Denaturing the protein tends to expose the chromophore to more solvent increase the total Stokes shift and increase the relative contribution of the ultra-fast component.

(ii) The different decay times observed for a particular system can vary by as many as four orders of magnitude, ranging from 10's fsec to a nsec.

(iii) The relative contributions of the ultra-fast (100's fsec) and slow (10's psec) response are often of the same order of magnitude, consistent with equation (15).

(iv) Even when the chromophores are inside the protein, the coupling of the chromophore to the solvent is large. For example, Prodan is in a hydrophobic pocket of HSA, well away from the surface, and yet $\alpha_s \sim 50$. Even for the "buried" chromophores (Leu[7] and Phe[30]) in GB1,[90] the solvent contribution is $A_s E_R \sim 100$ cm^{-1}, $\tau_s \sim 5$ psec, and so $\alpha_s \sim 100$. There are several proteins for which a very slow (~ 10's nsec) dynamic Stokes shift has been observed and has been assigned to dielectric relaxation of the protein itself[81, 82].

(v) The values of the dimensionless couplings α_j that we obtain from (51) are comparable to the rough estimates we made in Section I D.

Three pulse photon echo spectroscopy. This technique is analogous to stimulated spin echo measurements used in nuclear magnetic resonance to extract the phase relaxation time T_2. For "long" times it can be shown[85] that the

TABLE II: Solvation relaxation times for various chromophores in different protein and solvent environments. The values of relaxation times and their relative weights are determined by fitting the time dependence of the dynamic Stokes shift (47) to the functional form (49). E_R is the reorganisation energy, given by (6), and equals the total Stokes shift. Note there is some variation in estimates of the reorganisation energy depending on whether one estimates it from the maxima in the absorption and emission spectra or from the first frequency moment of the spectra [15]. It should be noted that the time resolution is different in the various experiments. Some did not have access to femtosecond time scales and so we have left the relevant columns blank. SC is Subtilisin Carlsberg. HSA is Human serum albumin. SNase-WT is Staphylococcus nuclease in the wild type. SNase-K110A is a specific mutant of Staphylococcus nuclease. HSA is in its native folded form in the buffer but denatures in concentrations of Gdn.HCl (guanidine hydrogen chloride) greater than about 5M and at a pH above 7. Trp is the amino acid Tryptophan, Acrylodan is 6-acryloyl-2-(dimethylamino)naphthalene, Prodan is 6-propionyl-2-(dimethylamino)naphthalene, AP is amino-pyridine, DCM is 4-(dicyanomethylene)-2-methyl-6-(p-dimethylaminostyryl) 4H-pyran, MPTS is 8-methoxypyrene-1,3,6-trisulfonate, and bis-ANS is 1,1-bis(4-anilino)naphthalene-5,5' disulfonic acid.

Chromophore	Protein	Solvent	Ref.	E_R (cm^{-1})	A_1, τ_1	A_2, τ_2	A_3, τ_3
Trp	none	water	[91]		0.65, 160 fsec	0.35, 1.1 psec	
Trp	none	water	[92]	2193	0.55, 340 fsec	0.45, 1.6 psec	
Trp	SC	buffer	[93]	1440	0.6, 800 fsec	0.4, 38 psec	
Trp	Monellin	buffer	[32]	960	0.46, 1.3 psec	0.54, 16 psec	
Trp	SNase-WT	buffer	[94]	850	0.46, 5 psec	0.54, 153 psec	
Trp	SNase-K110A	buffer	[94]	876	0.77, 3 psec	0.23, 96 psec	
Trp	HSA	water, pH 7	[95]	1156	0.39, 5 psec	0.61, 133 psec	
Trp	HSA	water, pH 9	[95]	1015	0.3, 1.6 psec	0.7, 46 psec	
Dansyl	SC	water	[93]	1180	0.94, 1.5 psec	0.06, 40 psec	
DCM	HSA	Tris buffer	[82]	515		0.25, 600 psec	0.75, 10 nsec
Prodan	none	buffer	[96]	2313	0.47, 130 fsec	0.53, 770 fsec	
Prodan	HSA	buffer	[96]	916	0.19, 780 fsec	0.56, 2.6 psec	0.25, 32 psec
Acrylodan	HSA	buffer	[96]	1680	0.23, 710 fsec	0.41, 3.7 psec	0.36, 57 psec
Acrylodan	HSA	0.2M Gdn.HCl	[96]		0.16, 280 fsec	0.36, 5.4 psec	0.48, 61 psec
Acrylodan	HSA	0.6M Gdn.HCl	[96]		0.2, 120 fsec	0.55, 2 psec	0.25, 13.5 psec
MPTS	none	buffer	[62]	2097	0.8, 20 fsec	0.2, 340 fsec	
MPTS	Ab6C8	buffer	[62]	1910	0.85, 33 fsec	0.1, 2 psec	0.05, 67 psec
bis-ANS	GlnRS (native)	water	[33]	750		0.45, 170 psec	0.55, 2.4 nsec
bis-ANS	GlnRS (molten)	urea	[33]	500		0.63, 60 psec	0.37, 0.96 nsec
4-AP	GlnRS (native)	water	[33]	1330		0.85, 40 psec	0.15, 580 psec
4-AP	GlnRS (molten)	urea	[33]	700		0.77, 50 psec	0.23, 0.9 nsec
Zn-porphyrin	Cytochrome-c	water	[97]	170		0.4, 250 psec	0.6, 1.5 nsec

time-dependent echo peak shift $S(t)$, where t is the time delay between the second and third pulse, is related to the correlation function $C(t)$, given in (48), by

$$S(t) = \frac{\tau_g}{\sqrt{\pi}} C(t) \tag{52}$$

where τ_g is the decoherence timescale given in eq. (22), and associated with the "collapse of the wave function."

The solvation dynamics of the fluorescein dye eosin bound to lysozyme in an aqueous solution was studied and compared to that for eosin in water without the protein[15]. For both systems, ultra-fast solvation relaxation occurs in about 10 fsec and is assigned to bulk water. However, for the lysozyme-eosin complex a slower relaxation also occurred on the scale of 100 psec. This was assigned as predominantly due to water bound to the protein, mostly in the first hydration shell. This can be compared with dielectric dispersion measurements [109] which suggest that there are two solvation relaxation times of 4 psec and 270 psec. A molecular dynamics simulation of lysozyme in an explicit solvent environment of 5345 water molecules found a single solvation relaxation time of 100 psec [98]. Jordanides *et al.*[15] used the dynamic dielectric continuum model of Song and Chandler [60] to extract the spectral density, based on four different dielectric models. The full time dependence of the solvation was best described by a model which included the frequency dependence of dielectric constant of both the lysozyme and the water bound at the protein surface. These models for the lysozyme complex can be compared to our models if some simplifying assumptions are made. In particular, we need to treat the lysozyme protein as spherical with the eosin complex at its centre. Models I and II in Ref. [15] then correspond to our Models 3 and 5, respectively. Models III and IV are approximately our Model 4, with the appropriate choice for the protein dielectric constant of the protein.

VI. COMPARISON WITH SPECTRAL DENSITIES DETERMINED FROM MOLECULAR DYNAMICS SIMULATIONS

For several specific proteins molecular dynamic simulations have been used to determine several quantities relevant to this work: the static dielectric constant of the protein, the frequency dependent dielectric constant, solvation dynamics, or the spectral density associated with an optical transition in a chromophore or an electron transfer. [3, 57, 76, 77, 98, 99, 100, 101, 102, 103, 104] We hope that our work will stimulate further simulations of the spectral density for specific chromophores and proteins in an aqueous environment. To determine it one needs to calculate time correlations of the (reaction field) electric field at the location of the chromophore within the protein. Equivalently, the spectral density can be related to the fluctuations in the energy difference between the ground and excited states of the system [99]. We now briefly review some of the results on specific proteins that are relevant to this paper.

A. Tryptophan in monellin and water

Molecular dynamics was used to calculate the time correlation function $C(t)$ for trajectories of a few nanoseconds [104]. For free Trp in bulk water $C(t)$ was fit to a bi-exponential decay function with $A_1 = 0.86 \pm 0.04, \tau_1 = 70 \pm 10$ fs, and $A_2 = 0.14 \pm 0.04, \tau_2 = 0.7 \pm 0.2$ ps. For Trp-3 in the protein monellin $C(t)$ was fit to a tri-exponential form with $A_1 = 0.66 \pm 0.02, \tau_1 = 70 \pm 10$ fs; $A_2 = 0.22 \pm 0.02, \tau_2 = 1.0 \pm 0.1$ps; $A_3 = 0.12 \pm 0.01, \tau_3 = 23 \pm 2$ psec. The total reorganisation energy was calculated as $E_R = 3200$ cm^{-1}. The two faster decays were assigned to the bulk water and the slowest component ($\tau_3 = 23 \pm 2$ ps) was assigned to protein dynamics including the motion of the chromophore within the protein. This assignment is consistent with the interpretation of NMR measurements but is different to that given in the associated experimental measurements [32] of the time dependent Stokes shift. The latter assigned the slower time scale (~ 20 psec) to the dynamic exchange between water bound at the protein surface (the first hydration shell) with bulk water.

B. Protein GB1 in water

The dynamic Stokes shift of a chromophore at the site of several different amino acid residues within the B1 domain of the protein G was measured.[90] The residues were replaced with an Aladin chromophore at sites that were "buried" (Leu[7] and Phe[30]), partially exposed (Trp[43]), and exposed(Ala[24]), to the solvent. The more exposed the site the larger the dynamic Stokes shift and the faster the relaxation. Motivated by these experiments, Golosov and Karplus performed molecular dynamic simulations for this 56 residue protein in a solvent of 6205 water molecules.[105] They calculated the time-dependent correlation function for the electrostatic interaction energy of the site residue with the rest of the system. This quantity should scale with the energy gap correlation function. For eleven different

sites the solvent coverage (defined as the ratio of the surface area of the residue that is accessible to the solvent to the surface area of the isolated residue) ranged from 5 to 45 per cent. The hydration correlation function was found to vary significantly between sites, but all contained components that could be assigned to ultra-fast decay (on the 100 fsec and 1 psec timescales, due to the surrounding water) and much slower relaxation (on the 100's psec timescale) that could be assigned to coupled hydration and protein conformational dynamics. However, there was no simple correlation between the slow relaxation time scale and the extent of the exposure of the site to the solvent, contrary to the correlation found by others.[106]

C.   Frequency dependent dielectric properties of an HIV1 zinc finger peptide in water

This peptide consisted of 18 amino acid residues and was simulated in a periodic box containing 2872 water molecules.[77] It was simulated for 13.1 nsec and exhibited a clear separation of time scales associated with dielectric relaxation of the different parts of the system. The water had a dielectric relaxation time of 7 psec, comparable to that for bulk water. Dielectric relaxation of the protein was dominated by a time scale of 4.3 nsec comparable to that found in simulations of other proteins and comparable to the time scale for rotation of the whole protein. The static dielectric constant of the peptide was estimated to be 15.

D.   Frequency dependent dielectric properties of ubiquitin in water

Ubiquitin is a small globular protein composed of 76 amino acids. It was simulated in a cubic box containing 5523 water molecules for runs of 5 nsec duration.[101] Time dependent correlation functions (which are the fourier transform of the frequency dependent dielectric constant) could be fit to sums of two decaying exponentials with different weights and relaxation times. For the dielectric relaxation the three dominant timescales observed were 7 psec, 2.6 nsec, and 1.9 nsec. These were associated with the bulk water, with rotation of the whole protein, and the bound water and side chains at the protein surface, respectively. Recently the same group extended the simulations to 20 nsec and also calculated the frequency dependent dielectric constant of solutions of the proteins apo-calbindin D_{9K} and the C-terminal domain of phospholipase C-γ1.[103]

VII.   CONCLUSIONS

The focus of this paper has been on the coupling of optical transitions in biological chromophores to their environment. However, the approach and results presented here can be readily adapted to other transitions involving two quantum states which differ in the value of their electric dipole moment. Examples include intersystem crossing, non-radiative decay via a conical intersection, electron transfer and proton transfer.

We hope our work will stimulate more work considering the following general claims, which this paper has elucidated.

(i) A valuable approach to modelling quantum dynamics in specific biomolecular systems may be in terms of "minimal" models such as the spin-boson model where the system parameters and spectral density are extracted from experiment and/or quantum chemistry and molecular dynamics.

(ii) Even when the active site of a biomolecule is shielded from bulk water, the latter can still have a significant effect on the quantum dynamics of the active site, especially if the time scale of interest is comparable to the solvation time scale associated with the bulk water. This can lead to solvent fluctuations dominating protein dynamics and function [83].

(iii) The environment of the active site can be divided into three distinct components: the surrounding protein, water at the protein surface, and bulk water. The times scales associated with the dielectric relaxation of each component usually differs by several orders of magnitude and so each makes a unique contribution the coupling of the quantum dynamics of the active site to the environment. Furthermore, the relative importance of each component depends on how the time (or energy) scale of the quantum dynamics, compares to time scale of the solvation associated with each of the components of the environment. Table 1 compares the associated energy scales.

(iv) The time scales associated with decoherence and the "collapse of the wave-function" in these biomolecular systems are experimentally accessible. Given the high tuneability of these systems they could potentially be used in fundamental studies concerning quantum measurement theory.

VIII.   ACKNOWLEDGEMENTS

[1] V. Helms, Curr. Opinion Struct. Bio. **12**, 169 (2002).

[2] M. Sarikaya, C. Tamerler, A. K.-Y. Jen, K. Schulten, and F. Baneyx, Nature Materials **270**, 577 (2003).

[3] A. Warshel and W. W. Parson, Quart. Rev. Biophys. **34**, 563 (2001).

[4] G. Groenhof, M. Bouxin-Cademartory, B. Hess, S. deVisser, H. Berendsen, M. Olivucci, A. Mark, and M. Robb, J. Amer. Chem. Soc. **126**, 4228 (2004), ISSN 0002-7863.

[5] J. Gilmore and R.H. McKenzie, Chem. Phys. Lett. **421**, 266 (2006).

[6] J. Gilmore and R.H. McKenzie, J. Phys.: Cond. Matt. **17**, 1735 (2005).

[7] J.T. Edsall and H.A. McKenzie, Adv. Biophys. **16**, 53 (1983).

[8] A. Wand, Nature Struct. Bio. **8**, 926 (2001).

[9] M. Vengris, M. A. van der Horst, G. Zgrablic, I. H. M. van Stokkum, S. Haacke, M. Chergui, K. J. Hellingwerf, R. van Grondelle, and D. S. Larson, Biophys. J. **87**, 1848 (2004).

[10] M. Zimmer, Chem. Rev. **102** (2002).

[11] C. Mattos, Trends in Biochem. Sci. **27**, 203 (2002).

[12] B. Halle, Philos. Trans. R. Soc. London B **359**, 1207 (2004).

[13] P. C. W. Davies, BioSystems **78**, 69 (2004); G. Fleming and G. Scholes, Nature **431**, 256 (2004); P. Ball, Nature **2004**, 396 (2004); C. Koch and K. Hepp, Nature **440**, 611 (2006); R. Sension, Nature **446**, 740 (2007).

[14] G. Engel, T. Calhoun, E. Read, T.-K. Ahn, T. Manal, Y.-C. Cheng, R. Blankenship, and G. Fleming, Nature **446**, 782 (2007).

[15] X. J. Jordanides, M. J. Lang, X. Song, and G. R. Fleming, J. Phys. Chem. B **103**, 7995 (1999).

[16] M. Chachisvilis, O. Kühn, T. Pullerits, and V. Sundström, J. Phys. Chem. B **101**, 7275 (1997).

[17] G. Trinkunas, J. L. Herek, T. Polívka, V. Sundström, and T. Pullerits, Phys. Rev. Lett. **86**, 4167 (2001).

[18] T. Brixner, J. Stenger, H. M. Vaswani, M. Cho, R. E. Blankenship, and G. R. Fleming, Nature **434**, 625 (2005).

[19] J. Herek, W. Wohlleben, R. Cogdell, D. Zeidler, and M. Motzkus, Nature **417**, 533 (2002).

[20] X. Hu, T. Ritz, A. Damjanovic, and K. Schulten, J. Phys. Chem. B **101**, 3854 (1997).

[21] T. Pullerits, M. Chachisvillis, and V. Sundström, J. Phys. Chem. **100**, 10792 (1996).

[22] R. Monshouwer, M. Abrahamsson, F. van Mourik, and R. van Grondelle, J. Phys. Chem. B **101**, 7241 (1997).

[23] I. Buchvarov, Q. Wang, M. Raytchev, A. Trifonov, and T. Fiebig, Proc. Nat. Acad. Sci. **104**, 4794 (2007).

[24] U. Genick, S. Soltis, P. Kuhn, I. Canestrelli, and E. Getzoff, Nature **392**, 206 (1998).

[25] B. M. Cho, C. F. Carlsson, and R. Jimenez, J. Chem. Phys. **124**, 144905 (2006).

[26] L. Y. Zhang and R. A. Friesner, Proc. Natl. Acad. Sci. **95**, 13603 (1998).

[27] J. R. Reimers and N. S. Hush, Chem. Phys. **208**, 177 (1996).

[28] T. Kawatsu, T. Kakitani, and T. Yamato, J. Phys. Chem. B **106**, 11356 (2002).

[29] D. Borgis and J. T. Hynes, J. Phys. Chem. **100**, 1118 (1996).

[30] M. Ben-Nun, F. Molnar, H. Lu, J. C. Phillips, T. J. Martínez, and K. Schulten, Faraday Discuss. **110**, 447 (1998).

[31] M. S. Lang, X. J. Jordanides, X. Song, and G. Fleming, J. Chem. Phys. **110**, 5884 (1999).

[32] J. Peon, S. K. Pal, and A. H. Zewail, Proc. Natl. Acad. Sci. **99**, 10964 (2002).

[33] P. Sen, S. Mukherjee, P. Dutta, A. Halder, D. Mandal, R. Banerjee, S. Roy, and K. Bhattacharyya, J. Phys. Chem. B **107**, 14563 (2003).

[34] U. Weiss, *Quantum dissipative systems* (World Scientific, Singapore, 1999), 2nd ed.

[35] A.J. Leggett, Science **871**, 307 (2005); J. Phys.: Cond. Matt. **14**, R415 (2002).

[36] M. Schlosshauer, Rev. Mod. Phys. **76**, 1267 (2004).

[37] W.H. Zurek, Phys. Today 44 (10), 36 (1991); an updated version is available as quant-ph/0306072; J.P. Paz and W.H. Zurek, quant-ph/0010011; W.H. Zurek, Rev. Mod. Phys. 75, 715 (2005).

[38] W. G. Unruh, Phys. Rev. A **51**, 992 (1995).

[39] I. Chuang, R. Laflamme, P. Shor, and W. Zurek, Science **270**, 1633 (1995).

[40] D. Xu and K. Schulten, Chem. Phys. **182**, 91 (1994).

[41] A. Garg, J. N. Onuchic, and V. Ambegaokar, J. Chem. Phys. **83**, 4491 (1985).

[42] K. E. van Holde, W. C. Johnson, and P. S. Ho, *Physical Biochemistry* (Prentice-Hall, 1998).

[43] C. Hettich, C. Schmitt, J. Zitzmann, S. Kühn, I. Gerhardt, and V. Sandoghdar, Science **298**, 385 (2002).

[44] O. Kühn, V. Sundström, and T. Pullerits, Chem. Phys. **275**, 15 (2002).

[45] N. Prokof'ev and P. Stamp, Rep. Prog. Phys. **63**, 669 (2000).

[46] F. Lesage and H. Saleur, Phys. Rev. Lett. **80**, 4370 (1998).
[47] E. Joos, Phys. Rev. D **29**, 1626 (1984); W. Zurek, Phys. Rev. D **26**, 1862 (1982). E. Joos and H. Zeh, Z. Phys. B **59**, 223 (1985); E. Joos, H. D. Zeh, C. Kiefer, J. Kupsch, and I. O. Stamatescu, *Decoherence and the Appearance of a Classical World in Quantum Theory* (Springer, 2003), 2nd ed.
[48] B. Carmeli and D. Chandler, J. Chem. Phys. **89**, 452 (1988).
[49] L. Muhlbacher and R. Egger, J. Chem. Phys. **118**, 179 (2003).
[50] R. Bulla, H.-J. Lee, N.-H. Tong, and M. Vojta, Phys. Rev. B **71**, 045122 (2005).
[51] S. Kehrein, A. Mielke, and P. Neu, Z. Phys. B **99**, 269 (1996).
[52] N. Niimura, S. Arai, K. Kurihara, T. Chatake, I. Tanaka, and R. Bau, in *Hydrogen- and Hydration-Sensitive Structural Biology*, edited by N. Niimura, H. Mizuno, J. R. Helliwell, and E. Westhof (2005), p. 17.
[53] S.K. Pal and A.H. Zewail, Chem. Rev. **104**, 2099 (2004).
[54] E. Grant, R. Sheppard, and G. South, *Dielectric behavior of biological molecules* (Oxford, Clarendon, 1978).
[55] N. Nandi and B. Bagchi, J. Phys. Chem. B **101**, 10954 (1997).
[56] K. Bhattacharyya, Acc. Chem. Res. **36**, 95 (2003).
[57] S. Höfinger and T. Simonson, J. Comp. Chem. **22**, 290 (2001).
[58] T. Simonson, Curr. Opinion Struct. Bio. **114**, 243 (2001).
[59] C.-P. Hsu, X. Song, and R. A. Marcus, J. Phys. Chem. B **101**, 2546 (1997).
[60] X. Song and D. Chandler, J. Chem. Phys. **108**, 2594 (1998).
[61] C. Cramer and D. Truhlar, Chem. Rev. **99**, 2161 (1999).
[62] R. Jimenez, D. Case, and F. Romesberg, J. Phys. Chem. B **106**, 1090 (2002).
[63] B. J. Homoelle, M. D. Edington, W. M. Diffey, and W. F. J. Beck, J. Phys. Chem. B **102**, 3044 (1998).
[64] R. E. Riter, M. D. Edington, and W. F. Beck, J. Phys. Chem. B **100**, 14198 (1996).
[65] G. D. Mahan, *Many-Particle Physics* (Plenum Press, New York and London, 1990), 2nd ed., Section 4.3.
[66] L. Onsager, J. Am. Chem. Soc. **58**, 1486 (1936).
[67] C. Bottcher, *Theory of electric polarization*, vol. 1 (Elsevier, Amsterdam, 1973).
[68] J. H. Reina, L. Quiroga, and N. F. Johnson, Phys. Rev. A **65**, 032326 (2002).
[69] G. Fleming and M. Cho, Annu. Rev. Phys. Chem. **47**, 109 (1996).
[70] D. Voges and A. Karshikoff, J. Chem. Phys. **108**, 2219 (1998).
[71] C. Schutz and A. Warshel, Proteins: Structure, Function, and Genetics **44**, 400 (2001).
[72] X. Song and R. Marcus, J. Chem. Phys. **99**, 7768 (1993).
[73] M. N. Afsar and J. B. Hasted, Infrared Phys. **18**, 835 (1978).
[74] M. L. Horng, J. A. Gardecki, A. Papazyan, and M. Maroncelli, J. Phys. Chem. **99**, 17311 (1995).
[75] J. T. Kindt and C. A. Schmuttenmaer, J. Phys. Chem. **100**, 10373 (1996).
[76] J. Pitera, M. Falta, and W. F. van Gunsteren, Biophys. J. **80**, 2546 (2001).
[77] G. Loffler, H. Schreiber, and O. Steinhauser, J. Mol. Biol. **270**, 520 (1997).
[78] R. S. Moog, A. Kiki, M. Fayer, and S. G. Boxer, Biochemistry **23**, 1546 (1984).
[79] H.-W. Trissl, K. Bernhardt, and M. Lapin, Biochemistry **40**, 5290 (2001).
[80] S. Pal, S. Balasubramanian, and B. Bagchi, J. Chem. Phys. **120**, 1912 (2004).
[81] W. Pierce and S. G. Boxer, J. Phys. Chem. **96**, 5560 (1992); M. Vincent, A. Gilles, I. de la Sierra, P. Briozzo, O. Barzu, and J. Gallay, J. Phys. Chem. B **104**, 11286 (2000); J. Lakowicz, Photochem. Photobiol. **72**, 421 (2000); A. Toptygin, D. Gronenborn, and L. Brand, J. Phys. Chem. B **110**, 26292 (2006).
[82] S. K. Pal, D. Mandal, D. Sukul, S. Sen, and K. Bhattacharyya, J. Phys. Chem. B **105**, 1438 (2001).
[83] P. Fenimore, H. Frauenfelder, B. McMahon, and F. G. Parak, Proc. Natl. Acad. Sci. **99**, 16047 (2002); P. Fenimore, H. Frauenfelder, B. McMahon, and R. D. Young, Physica A **351**, 1 (2005); V. Lubcheno, P. Wolynes, and H. Frauenfelder, J. Phys. Chem. B **109**, 7488 (2005).
[84] J. T. M. Kennis, D. S. Larsen, K. Ohta, M. T. Facciotti, R. M. Galeser, and G. R. Fleming, J. Phys. Chem. B **106**, 6067 (2002).
[85] W.P. de Boej, M.S. Pshenichnikov, and D.A. Wiersma, J. Phys. Chem. **100**, 11806 (1996); Annu. Rev. Phys. Chem. **49**, 99 (1998).
[86] R. Jimenez, G. Fleming, P. Kumar, and M. Maroncelli, Nature **369**, 471 (1994).
[87] P. Changenet-Barret, C. Choma, E. Gooding, W. DeGrado, and R. Hochstrasser, J. Phys. Chem. B **104**, 9322 (2000).
[88] R. Jimenez, G. Salazar, K. Baldridge, and F. Romesberg, Proc. Natl. Acad. Sci. **100**, 91 (2003).
[89] R. Jimenez, G. Salazar, Y. Jina, T. Hoo, and F. E. Romesberg, Proc. Natl. Acad. Sci. **101**, 3803 (2004).
[90] B. E. Cohen, T. B. McAnaney, E. S. Parl, Y. N. Jan, S. G. Boxer, and L. Y. Jan, Science **296**, 1700 (2002).
[91] D. Zhong, S. K. Pal, D. Zhang, S. I. Chan, and A. H. Zewail, Proc. Natl. Acad. Sci. **99**, 13 (2002).
[92] W. Lu, J. Kim, W. Qiu, and D. Zhong, Chem. Phys. Lett. **388**, 120 (2004).
[93] S. K. Pal, J. Peon, and A. H. Zewail, Proc. Natl. Acad. Sci. **99**, 15297 (2002).
[94] W. Qiu, Y.-T. Kao, L. Zhang, Y. Yang, L. Wang, W. Stites, D. Zhong, and A. Zewail, Proc. Natl. Acad. Sci. **103**, 13979 (2006).
[95] W. Qiu, L. Zhang, O. Okobiah, Y. Yang, L. Wang, D. Zhong, and A. Zewail, J. Phys. Chem. B **110**, 10540 (2006).
[96] J. K. A. Kamal, L. Zhao, and A. H. Zewail, Proc. Natl. Acad. Sci. **101**, 13411 (2004).
[97] S. Lampa-Pastirk and W. Beck, J. Phys. Chem. B **108**, 16288 (2004).
[98] P. Smith, R. Brunne, A. Mark, and W. V. Gunsteren, J. Phys. Chem. **97**, 2009 (1993).
[99] D. Xu and K. Schulten, in *The Photosynthetic Bacterial Reaction Center: II. Structure, Spectroscopy and Dynamics,*

edited by J. Breton and A. Vermeglio (Plenum Press, 1992), p. 301.

[100] I. Kosztin and K. Schulten, in *Molecular dynamics methods for bioelectronic systems in photosynthesis*, edited by T. Aartsma and J. Matysik (Kluwer Academic Publishers, in press).

[101] S. Boresch, P. Höchtl, and O. Steinhauser, J. Phys. Chem. B **104**, 8743 (2000).

[102] O. Miyashita and N. Go, J. Phys. Chem. B **104**, 7516 (2000).

[103] T. Rudas, C. Schröder, S. Boresch, and O. Steinhauser, J. Chem. Phys. **124**, 234908 (2006).

[104] L. Nilsson and B. Halle, Proc. Natl. Acad. Sci. **102**, 13867 (2005).

[105] A. Golosov and M. Karplus, J. Phys. Chem. B **111**, 1482 (2007).

[106] S. Bandyopadhyay, S. Chakraborty, S. Balasubramanian, and B. Bagchi, J. Am. Chem. Soc. **127**, 4071 (2005).

[107] B. Bagchi, Annu. Rep. Prog. Chem., Sect C **99**, 127 (2003).

[108] K. Yoshiba, A. Teramoto, N. Nakamure, T. Shikata, Y. Miyazaki, M. Sorai, Y. Hayashi, and N. Miura, Biomacromolecules **5**, 2137 (2004).

[109] S. C. Harvey and P. Hoekstra, J. Phys. Chem. **76**, 2987 (1972).

APPENDIX A: TIMESCALES

TABLE III: Timescales for various processes in biomolecules and solutions. The radiative lifetime of a chromophore is order of magnitudes longer than all other timescales, except perhaps protein dielectric relaxation. MD refers to results from molecular dynamics simulations. Of particular relevance to this work is the separation of timescales, $\tau_s \ll \tau_b \ll \tau_p$ (compare Fig. 2).

Process	Timescale	Ref.
Radiative lifetime	10 ns	[42]
Internal conversion	10fs	[42]
Bulk water dielectric relaxation	8 ps	[73]
Protein dielectric relaxation (MD), $\tau_{D,p}$	1-10 ns	[77, 101]
Ultrafast solvation in water	10's fs	[31]
Fast solvation in water, τ_s	100's fs	[31]
Solvation due to bound water, τ_b	5-50 ps	[32]
Solvation due to protein, τ_p	1-10 ns	[33]
Covalent bond vibrations	10-100 fs	[42]
Elastic vibrations of globular regions	1-10 ps	[42]
Rotation of surface sidechains	10-100 ps	[42]
Reorientation of whole protein	4-15 ns	[101]

APPENDIX B: SOLUTION FOR THE REACTION FIELD

A change in the dipole moment of the chromophore leads to a re-organisation of the environment, which produces a reaction field acting back on the dipole. This is shown schematically in Figure 4.

The reaction field for these models can be obtained by a generalisation of the techniques in ref. [67] as follows: The electric potential, $\phi(x,y,z)$, satisfies Poisson's equation $\nabla^2\phi = -\rho/\epsilon$, where ϵ is the local dielectric constant of the medium and ρ is the local charge density. Away from the point dipole and surface boundaries, $\rho = 0$ and we must solve Laplace's equation $\nabla^2\phi = 0$. At the dielectric boundaries (and in general), ϕ must be continuous and because there are no free charges, $\vec{D} = \epsilon\vec{E} = -\epsilon\nabla\phi$ is also continuous across the boundaries.

Although the protein is spherically symmetric, because of the point-dipole, the system has only cylindrical symmetry. If the spherically symmetric electric potential in each concentric dielectric shell is given by $\phi_1(r), \phi_2(r), \ldots$, we can expand ϕ_i in terms of spherical harmonics [67]:

$$\phi_i = \sum_{n=0}^{\infty} \left(A_{i,n} r^n + \frac{B_{i,n}}{r^{n+1}} \right) P_n(\cos\theta)$$

We consider explicitly the case where we have a cavity surrounded by a single dielectric shell inside a bulk solvent. The central cavity has radius a, dielectric ϵ_c and potential $\phi_c(r,\omega)$, the shell has total radius b (thickness $b - a$), dielectric ϵ_p and potential $\phi_p(r,\theta)$, and the bulk environment is described by dielectric ϵ_e and potential $\phi_e(r,\omega)$.
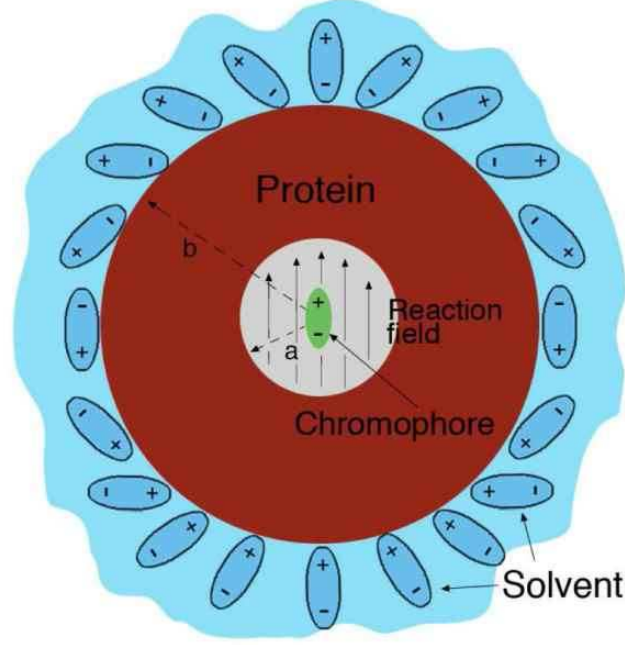
FIG. 4: Model 4 for the interaction between a chromophore and its environment. The chromophore is treated as a point dipole sitting in a cavity of radius a in the centre of a spherical, uniform protein which is treated as a homogeneous dielectric medium of radius b. The protein-pigment complex is surrounded by a solvent, typically water, which is again treated as a homogeneous dielectric medium though actual molecules are shown for clarity of explanation. The chromophore's dipole moment polarises its environment, which in turn produces an electric field, the "reaction field", which interacts with the chromophore. Fluctuations in the environment will translate to fluctuations in the chromophore's energy.

We can then apply the boundary conditions:

$$\phi_e(r \to \infty) \to 0 \tag{B1a}$$

$$\phi_\mu = \frac{\mu}{r^2} \cos \theta \tag{B1b}$$

$$(\phi_p)_{r=b} = (\phi_e)_{r=b} \tag{B1c}$$

$$(\phi_c)_{r=a} = (\phi_p)_{r=a} \tag{B1d}$$

$$\epsilon_c \left(\frac{\partial \phi_c}{\partial r} \right)_{r=a} = \epsilon_p \left(\frac{\partial \phi_p}{\partial r} \right)_{r=a} \tag{B1e}$$

$$\epsilon_p \left(\frac{\partial \phi_p}{\partial r} \right)_{r=b} = \epsilon_e \left(\frac{\partial \phi_e}{\partial r} \right)_{r=b} \tag{B1f}$$

The first condition is that the potential must go to zero at infinity. This means that all coefficients with positive powers of r must vanish, i.e., $A_{e,n} = 0$ for all n.

The second condition is the field from a point dipole. As this is the only free charge in the cavity, this is the only source term (inverse power of r) that will contribute to the potential $\phi(r,\theta)$. Since $P_1(\cos \theta) = \cos \theta$, only the $n = 1$ term is involved. Therefore, $B_{c,n=1} = \mu$ and $B_{c,n \neq 1} = 0$. (Nothing is said about $A_{c,n}$).

The final terms describe the continuity of the potential and its derivative over the boundary. The first condition gives

$$\sum_{n=0}^{\infty} \left(A_{p,n} b^n + \frac{B_{p,n}}{b^{n+1}} \right) P_n(\cos \theta) = \sum_{n=0}^{\infty} \frac{B_{e,n}}{b^{n+1}} P_n(\cos \theta) \tag{B2}$$

Because the spherical harmonics P_n are orthogonal, we can consider each term of this sum as being equal, so

$$A_{p,n} b^n + \frac{B_{p,n}}{b^{n+1}} = \frac{B_{e,n}}{b^{n+1}} \tag{B3}$$

In a similar way, the remaining boundary conditions can be applied to produce a set of linear equations on the $A_{i,n}$ and and $B_{i,n}$. We have six boundary conditions and six variables (each, of course, a function of n) and so we are able to solve for all parameters. However, we are only interested in the field inside the cavity, and in particular the unknown part $A_{c,n}$. We find that all the $A_{c,n}$ are zero except for $n = 1$. Thus, the potential due to the surface charges is given by $\phi_{c,\text{surf}} = -\chi\mu r\cos\theta = -\chi\mu\hat{z}$ where we find

$$\chi(\omega) = \frac{2}{a^3}\frac{(\epsilon_p + 2\epsilon_c)(\epsilon_e - \epsilon_p)a^3 + (\epsilon_p - \epsilon_c)(2\epsilon_e + \epsilon_p)b^3}{2(\epsilon_p - \epsilon_c)(\epsilon_e - \epsilon_p)a^3 + (2\epsilon_p + \epsilon_c)(2\epsilon_e + \epsilon_p)b^3} \tag{B4}$$

The actual electric field in the cavity due to the surface charges but not the dipole itself – the reaction field – is then $\vec{R} = R\hat{z} = -\nabla\phi_{e,\text{surf}}(x, y, z) = \chi\mu\hat{z}$, which will be a constant throughout the cavity, parallel to the dipole, and proportional to the dipole moment μ. The spectral density describing coupling of changes in the chromophore state to this environment is related to the zero temperature fluctuations in the reaction field [6]:

$$J(\omega) = (\Delta\mu)^2\text{Re}\int dt\, e^{i\omega t}\,\langle R(t)R(0)\rangle_{T=0} \tag{B5}$$

This can be shown by writing the reaction field $R(t)$ in terms of its normal modes' creation and annihilation operators. $\Delta\mu$ is the change in chromophore dipole moment on the transition from the ground to excited states. The fluctuations in the reaction field $\langle R(t)R(0)\rangle$ are obtained [6] from the fluctuation dissipation theorem, and are proportional to the imaginary part of $\chi(\omega)$ in (B4) above, yielding

$$J(\omega) = 2(\Delta\mu)^2\text{Im}(\chi(\omega)) \tag{B6}$$

Note the use of zero temperature fluctuations is a mathematical derivation only, and provided the appropriate temperature parameters for the solvent and protein are used, the resulting spectral density is applicable to all temperatures.